Journal Pre-proof

Selective production of Dihydroxyacetone and Glyceraldehyde by Photo-assisted Oxidation of Glycerol

Arisbeht Mendoza, Rubí Romero, Galilea P. Gutiérrez-Cedillo, Gustavo López-Tellez, Omar Lorenzo-González, Rosa María Gómez-Espinosa, Reyna Natividad

PII: S0920-5861(19)30532-2

DOI: https://doi.org/10.1016/j.cattod.2019.09.035

Reference: CATTOD 12488

To appear in: *Catalysis Today*

Received Date: 5 March 2019

Revised Date: 12 September 2019

Accepted Date: 23 September 2019

Please cite this article as: Mendoza A, Romero R, Gutiérrez-Cedillo GP, López-Tellez G, Lorenzo-González O, Gómez-Espinosa RM, Natividad R, Selective production of Dihydroxyacetone and Glyceraldehyde by Photo-assisted Oxidation of Glycerol, *Catalysis Today* (2019), doi: https://doi.org/10.1016/j.cattod.2019.09.035

Selective production of Dihydroxyacetone and Glyceraldehyde by Photo-assisted Oxidation of Glycerol

Arisbeht Mendoza, Rubí Romero*, Galilea P. Gutiérrez-Cedillo, Gustavo López-Tellez, Omar Lorenzo-González, Rosa María Gómez-Espinosa, Reyna Natividad*

Centro Conjunto de Investigación en Química Sustentable, UAEM-UNAM, Universidad Autónoma del Estado de México, Mexico, km 14.5 Toluca-Atlacomulco-Road, CP 50200

Corresponding authors e-mail: rnatividadr@uaemex.mx, rromeror@uaemex.mx, +52 722 2766610, Ext.7723.

Graphical abstract

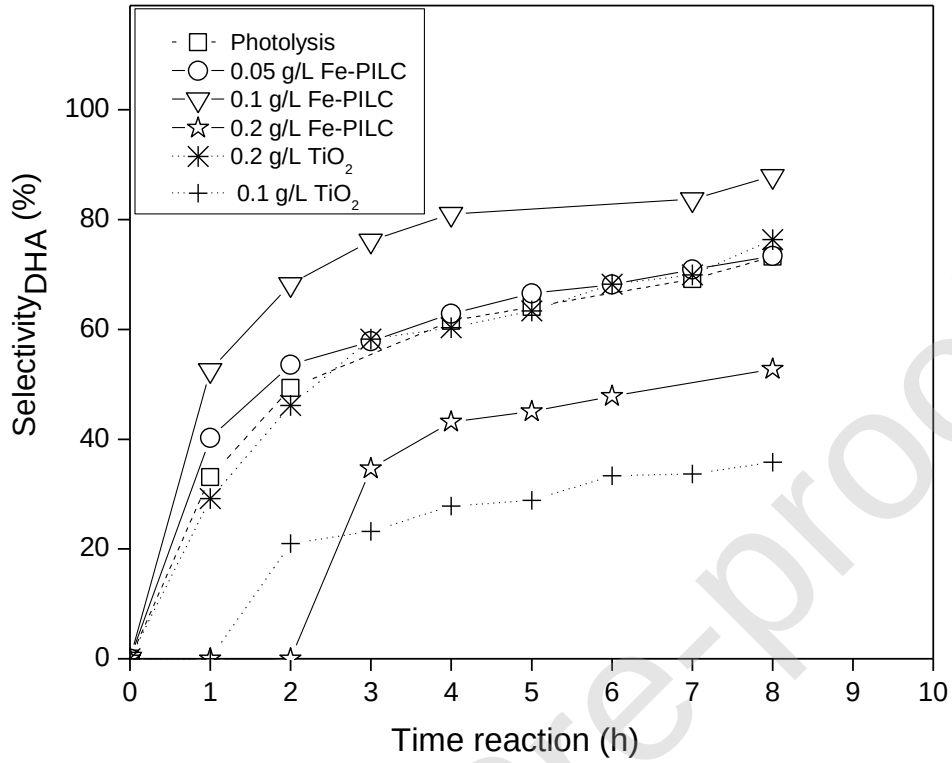

(a)

HIGHLIGHTS

- Fe-PILC enhances photo-oxidation of glycerol towards didhydroxyacetone
- Fe-PILC aids to conduct selective oxidations
- H_2O_2 is produced during glycerol photo-oxidation

Abstract

Glycerol is a by-product during biodiesel production and represents a potential low-cost raw material for obtaining high-cost products like Dihydroxyacetone (DHA) and glyceraldehyde (GCD) amongst others. In this work, Fe-Pillared clay (Fe-PILC) was assessed as catalyst of the selective photo-oxidation of glycerol to obtain DHA and GCD at moderate conditions (298 K and atmospheric pressure). This was conducted in a 100 mL Pyrex glass batch reactor where a Pen-Ray

lamp of mercury of 5.5 Watts UV light (UVP) was placed at the centre. The Fe-PILC was prepared by ion exchange. The pillaring was confirmed by XRD, and a 17% w/w of Fe was determined by Atomic Absorption Spectroscopy. The active phases were established by XPS and found to be FeO and Fe_3O_4. The specific surface area of the clay (bentonite), determined by N_2 physisorption, increased from 34 m^2/g to 227 m^2/g and the pore volume increased from 0.058 cm^3/g to 0.106 cm^3/g. The studied variables were catalyst loading and glycerol initial concentration. An experiment with TiO_2 Degussa P25 was also performed as reference. It was found that by adding Fe-PILC to the glycerol oxidation system, selectivity towards DHA or GCD can be tuned. A selectivity towards DHA was found to be 87% with 0.1 g/L of Fe-Pillared after 8 h reaction. The *in situ* production of H_2O_2 was observed and therefore concluded that the glycerol oxidation occurs via a fenton process, i.e. via free radicals.

Keywords

Photocatalysis, Fe-PILC, selective oxidation, Fenton, H_2O_2 production, H_2O_2 dissociation

1. Introduction

In recent years, the energy demand has increased due to urbanization and rapid population growth. As a result of this potential demand and to the problem of climate change due to the use of fossil fuels, it becomes imperative to find sustainable solutions in the short and medium term, such as biofuels (biodiesel). Biodiesel is considered an important alternative source of energy and it is the best candidate to be used in diesel engines for transport and heavy machinery without having to make major changes in them, in addition to advantages such as high biodegradability, reduction of carbon monoxide and oxide emissions of nitrogen, in its combustion organic aromatic products are not generated, decreases the emission of solid particles and the greenhouse effect, does not contain sulfur and it is highly biodegradable in water [1]. The glycerol or glycerin is one by-product from production of biodiesel (10 wt % of biodiesel is glycerol with a purity between 80-88%) and the estimated global production of biodiesel for 2018 is 35405 millions of liters and forecast value for 2023 is 40259 millions of liters [2], which translates to 4025 millions of liters of glycerol produced

in the market. With this potential increase in the amount of crude glycerol is necessary to have various methods for the elimination and/or use of the crude glycerol. To cope with excess glycerol, it is necessary to develop innovative and ecological catalytic processes to convert glycerol into higher economic value products, which is essential for the present and future of the crude glycerol market. The new applications of crude glycerol can indirectly help reduce the production costs of biodiesel and turn glycerol into a fundamental part of renewable energy. Nowadays, glycerol has been used in livestock feed, biogas, thermo-chemical products, combustion and as additive of pharmaceutics and cosmetics products [3]. Nevertheless, the crude glycerol obtained from the production of biodiesel contains many impurities (alcohol, organic or inorganic salts, water, glycerides traces, soap and catalysts). Therefore, the purification of crude glycerol is required if it is to be used in the pharmaceutical, cosmetic and food industries. These industries require purities up to 95 and 99% [4]. The purification of crude glycerol to above 99% for use in the pharmaceutical, food or cosmetic industries, is an expensive process [3]. Therefore, it is necessary to find new applications where the unrefined glycerol can be used, and in this way, obtain added value products. This could notably increase the economic aspect of overall biodiesel production, providing new applications and outlets for large quantities of crude glycerol obtained from biodiesel industry.

The interest on obtaining value-added products have motivated to study several pathways of degradation using selective catalysts towards some specific products. Some promising routes for the valorization of glycerol are: dehydration, hydrogenolysis, dehydroxylation, polycondensation, selective oxidation and fermentation [5–7].

Oxidation processes are the most commonly assessed to convert glycerol in a large number of high-value added products such as: glyceraldehyde (GAD), dihydroxyacetone (DHA), hydroxyl pyruvic acid, glyceric acid, tartronic acid, glycolic acid, glyoxylic acid, oxalic acid and formic acid [8,9]. Within these compounds, Dihydroxyacetone (DHA) occupies a very important place in the market, due to its use in the pharmaceutical and cosmetic industry. Also, it is used as a monomer in polymeric biomaterials [10]. Because of its use in the food industry, another important compound is

Glyceraldehyde (GAD) and is produced by the oxidation of the primary hydroxyl groups of glycerol. In order to improve the selectivity towards either of these compounds and the sustainability of the whole process, different strategies have been assessed. In this context, a promising approach has been heterogeneous photocatalysis since allows the use of atmospheric conditions and relative low-cost oxidizing agents such as air, oxygen and peroxide to conduct the selective oxidation of glycerol [11]. The most commonly assessed catalyst has been TiO_2 and the main studied variables are the type and the percentage of doping elements such as Au, Pt and Pd, with the disadvantage that they are deactivated at high reaction times, as a consequence of oxygen poisoning [10,12]. It has been shown that these variables and reaction conditions have a significant influence on the selectivity attained towards a specific product.

Thus, it is the aim of this work to assess the plausibility and effect of using iron-pillared clays (Fe-PILC) to conduct the photo-assisted selective oxidation of glycerol towards DHA. This catalyst has been proven to be effective on enhancing oxidation processes conducted by photo-fenton [13]. Interestingly enough, in this work, the addition of hydrogen peroxide was not necessary to conduct the partial oxidation of glycerol, but it was produced *in-situ* and its dissociation was catalyzed by Fe-PILC.

2. Experimental Section

2.1 Reagents

The reagents used for the synthesis of pillared clays were: Bentonite (pure-grade) supplied by Fisher Scientific with a >2 μm particle size and a cation exchange capacity of 94 meq/100g, Ferric Chloride Hexahydrate ($FeCl_3 \cdot 6H_2O$ with purity of 98.7%, Fermont), Sodium hydroxide (NaOH, 98.6%, Fermont), hydrochloric acid (37%) and deionized water (HYCEL). For the atomic absorption analysis, a Fe standard solution obtained from Spectro pure was utilized. To conduct the photocatalytic experiments, anhydrous glycerol ($C_3H_5(OH)_3$, 99.9%) supplied by J.T.Baker was

employed and for the analysis of products, standards provided by Sigma-Aldrich (glyceraldehyde and dihydroxyacetone) were utilized.

2.2 Synthesis and catalyst characterization

The method used for the catalyst synthesis has been described in detail by Valverde and Martín del Campo [13,14] and is summarized here as follows: 300 mL of aqueous solution of ferric chloride Hexahydrated (0.2M) was dropwise added to 600 mL of aqueous sodium hydroxide solution (0.2 M) under continuous stirring, after that the new solution was kept for further 4 hours under continuous stirring and pH of 1.8 ± 0.02 by using hydrochloric acid (5 M). The resulting solution was dropwise added to 1000 mL clay suspension (0.1% wt) under stirring, the final solution was aged at room temperature and the stirring continued for further 18 hours. Afterwards, the solid was obtained by filtration and washed with distilled and deionized water, dried overnight at 75 °C and calcined for 2h at 400°C. The catalyst was then labeled as Fe-PILC and characterized by X-ray Diffraction (XRD), Atomic Absorption Spectroscopy (AAS), N_2 Physisorption and X-ray Photoelectron Spectroscopy (XPS).

The XPS spectra of the Fe-PILC were obtained in a Photoelectron spectrometer Jeol JPS 9200 (standard MG-Kα excitation source (1253.6 eV) and binding energies were calibrated with regarding to carbon signal (C 1s) at 285 eV). XRD analysis was conducted in a Bruker Advance 8 equipment (Cu-Kα radiation at 35 kV and 30 mA and collection was conducted from 0 to 40° (2θ) with a step of 0.004°/min). For the AAS analysis, a catalyst sample was diluted with a HF solution and analyzed with an AA240FS VARIAN spectrometer. This was conducted in order to establish the real iron content in the prepared material. The specific surface areas of bentonite and Fe-PILC were calculated by nitrogen physisorption and this was carried out in a Quantachrome Autosorb analyzer (adsorption relative pressure P/Po=0.99 and 77° K, degassing conditions at 250°C for 2h under vacuum of 6.6 $x10^{-9}$ bar).

2.3 Selective photo-oxidation of glycerol

A jacketed Pyrex glass batch photoreactor was used for evaluation of Fe-PILC in the photo-oxidation of glycerol. The reactor dimensions were 20 cm of height and 2.5 cm of inner diameter. Inside, at the center of the reactor, an UVP Pen-Ray lamp of mercury of 5.5 Watts UV light was placed. This lamp emits primary energy at 254 nm with a typical intensity of 4400 μW/cm^2 and uses a power supply of 115 V/60 Hz. All experiments were conducted under continuous stirring and temperature was kept constant at 298 K by means of a cooling jacket.

For the reaction, firstly, 100 mL of solution of glycerol were loaded into the photoreactor along with a specific amount of Fe-PILC, immediately the lamp was turned on and the reaction started. The investigated variables were catalyst loading and type of catalyst. When catalyst loading was assessed, the experiments were performed with a 0.1M glycerol solution and four different Fe-PILC loadings were assessed: 0, 0.05, 0.1, and 0.2 g/L under T= 298±2 K and atmospheric pressure of 0.77 atm. With a catalyst loading of 0.2 g/L, the effect of type of catalyst (Fe-PILC and TiO_2 Degussa P25) was studied. An experiment with TiO_2 Degussa 25 was conducted in order to have as reference results obtained with a typical photocalyst.

1 mL samples were taken at different reaction times and centrifuged to remove the catalyst, after that they were filtered with a Thermo Scientific filter of 30 mm Nylon of 0.2μm for analysis by Ultra high-Performance Liquid Chromatography (UHPLC). Once the concentration of products was determined, the selectivity was calculated by means of Eq. 1,

$$S_i = \frac{mM_i}{mM_i + mM_j} * 100 \qquad \text{Eq. 1}$$

where S_i= selectivity of compound i (dihydroxyacetone or glyceraldehyde), mM

2.4 Analytical methods

The products generated by photo-oxidation of glycerol using Fe-PILC were analyzed by ultrahigh performance liquid chromatography (UHPLC). The equipment used for this purpose was a Thermo

Scientific Vanquish with a refractive index detector (RefractoMax520, Thermo Scientific). A Carbomix H NP 5: 8% (4.6 x 300, 5µm Non-Porous) column was used at 353 K. A mobile phase consisting of H_2SO_4 solution (10 mM) at constant flow rate of 0.26 mL/ min was employed. The reaction products were identified and quantified with the corresponding calibration curves. All measurements were conducted by triplicate and an error of 2% was established.

3. Results

3.1 Fe-PILC characterization

Figure 1 shows the diffractogram of the synthesized Fe-PILC. The diffractogram of the bentonite clay prior the pillaring process was also obtained. This is not shown here since has already been published somewhere else [13]. Figure 1 is the evidence that pillaring process was successfully conducted. The resulting basal spacing was 21.43 A. This is specifically indicated by the reflection d_{001} that appears at low angles (2θ=3°-4°) in figure 1, this is the evidence of the basal spacing enlargement characteristic when the metal becomes a pillar [13–15]. On the other hand, the presence of peaks at around 6° to 10° could give evidence that the species are intercalated in an irregular manner [16]. Reflections at around 21° and 27° are characteristic of bentonite [15]. There can also be observed in figure 1 some reflections that might be ascribed to magnetite and goethite. The results show an increase in surface area and pore volume after the pillaring process. Regarding surface area, this increased from 34 m^2/g to 227 m^2/g and the pore volume increased from 0.058 cm^3/g to 0.106 cm^3/g. This can be ascribed to the pillars formed among the clay layers [17]. Figure 2 depicts the XPS spectra and two deconvolution curves are shown. They were obtained from the binding energy corresponding to Fe $2p_{3/2}$. According to the National Institute of Standards and Technology (NIST), the first deconvolution curve corresponds to Fe_3O_4 (709.2 eV) and the second one can be ascribed to Fe^{2+} in FeO (709.6 eV).

3.2. Selective photo-oxidation of glycerol

3.2.1. Effect of catalyst loading and catalyst type

The study of this variable is rather important since allows to elucidate whether or not a heterogeneous process is being under the control of transport phenomena or under the control of the surface reactivity. It also dictates the product distribution of a consecutive/parallel reaction system [18–20]. In this context, figure 3 shows the DHA and GCD concentration profiles depending on time and Fe-PILC loading. Photolysis was included as reference and is considered as zero catalyst loading. The obtained results with TiO_2 at two catalyst loadings, 0.1 and 0.2 g/L, are also presented in figure 3.

Within glycerol photo-catalyzed oxidation related literature [21], it seems that the effect of UV light on glycerol molecule has been underestimated. In this work, however, we observed that both, DHA and GCD, were generated by only irradiating the 0.1 M glycerol solution without the addition of any catalyst. These results are shown in Fig. 3 and it can be observed that the accumulated concentration of DHA over 8 hours of reaction was 0.22 mM (20.04 mg/L). GCD, however, exhibits a rather different behavior since its concentration reaches a stationary state after only 1 hour of reaction at 0.08 mM (7.3 mg/L). This indicates that at this point, the rate of GCD accumulation becomes negligible and this implies that GCD is being consumed at the same rate that is being produced. GCD might be converting to other oxidation products like glycolic and glyceric acid. It can also be observed that during the first hour of reaction, GCD production rate (0.07×10^{-3} mol/L·h) is about twice faster than DHA one (0.035×10^{-3} mol/L·h). This is expected since the reactivity of the OH in C1 is higher than in C2 and thus the first hydrogen abstraction is light driven. It is also observed that the temporal DHA and GCD profiles obtained with TiO_2 are rather similar to those obtained by photolysis (figure 3). Actually, the DHA temporal profile is practically the same with TiO_2 than with light only. This was observed only when a TiO_2 loading of 0.2 g/L is employed, however, when a lower titania loading is used (0.1 g/L) a lower DHA concentration is achieved. This suggests that at low concentrations, titania competes for photons with glycerol and this negatively affects glycerol selective oxidation towards DHA (figure 3a).

It is also observed in figure 3, that both, DHA and GCD concentration profiles depend on Fe-PILC loading. The DHA concentration profile obtained at low catalyst loading, i.e. 0.05 g/L, shown in figure 3 a), suggests that the Fe-PILC does not compete with the effect of light and apparently does not exhibit any photo-activity. Furthermore, the effect of this solid seems to worsen GCD production compared to photolysis (Fig. 3b). However, a further increase in the catalyst loading leads to an increase in DHA concentration and selectivity towards this compound (Figure 4a). The highest DHA concentration (0.54mM) is observed with the catalyst loading of 0.1 g/L and this can be ascribed to the generation of hydroxyl radicals by means of reaction of eq.1 [22],

$$Fe^{3+} + H_2O + hv \rightarrow Fe^{2+} + \cdot OH + H^+ - - - (1)$$

Fig 3b) shows the concentration profiles of GCD obtained with different catalyst loading. In this graph it can be observed that the catalyst loading of 0.2 g/L does not follow the same trend with respect to the others. This behavior can be attributed to the prevailing reaction mechanism, when glycerol is in contact with Fe may be forming a ligand with the ·OH of the third carbon of glycerol, which by photons absorption produces GCD [23,24], where the limiting step can be the desorption of the products to the bulk fluid. The production of GCD was 0.15mM after 8 h of reaction. In the other reactions shown in Fig 3 b), it is observed that the production of GCD is kept constant and this behavior could be due to the transformation of GCD to other products such as glycolic acid which was identified but not quantified due to the very low observed signal.

It can also be observed that with 0.05 g/L, the formation of GCD is lower than under photolysis. This is suggesting that the addition of the Fe-PILC is limiting the photons usage by glycerol. This supports the statement that the initial stage of the glycerol oxidation is light driven and consists in the hydrogen abstraction (Scheme 1). This can subsequently react with oxygen from the medium (reaction 2) and form the hydroperoxyl radical that may lead to form hydrogen peroxide by reaction 3,

$$\cdot H + O_2 \rightarrow HO_2^{\cdot} - - - - - - - - (2)$$

$$HO_2^{\cdot} + HO_2^{\cdot} \rightarrow H_2O_2 + O_2 ----(3)$$

Actually, the *in-situ* production of hydrogen peroxide was verified and its evolution was established when using 0.2 g/L of Fe-PILC. This was plotted in figure 4. The generation of Hydrogen Peroxide during the photo-oxidation of glycerol was evaluated using a colorimetric method [25], that consisted on the formation of pertitanic acid (410 nm). Once H_2O_2 is produced, its dissociation is expected to readily occur via UV light action (reaction 4) and by the catalytic action of Fe^{2+} (reaction 5) [26],

$$H_2O_2 + h\nu \rightarrow 2OH^{\bullet} \quad (4)$$

$$Fe^{2+} + H_2O_2 \rightarrow Fe^{3+} + OH^- + OH^{\bullet} \quad (5)$$

Thus, as depicted in scheme 1, the production of GCD and DHA will be limited by the generated hydroxyl radicals, i.e. produced H_2O_2 (Fig. 4).

Regarding selectivity, it can be observed in figure 5 that selectivity towards DHA or GCD is not only a function of time but also of catalyst loading and catalyst type. In any case, it can be concluded that Fe-PILC, at the studied conditions, outperforms Degussa P25 since a higher selectivity towards DHA and glyceraldehyde is obtained via the Fenton process. In this sense, it is worth noticing that the selectivity towards DHA or GCD depends on the catalyst loading and this suggests that at the end what is influencing the product distribution is the concentration of reactive oxidant species. This is in concordance with that previously reported [27]. On the other hand, the results obtained with any of the TiO_2 loadings, showed less intermediaries production than Fe-PILC, and this can be due to a different oxidation mechanism [11,27].

3.2.2 Effect of initial glycerol concentration.

Two initial concentration of glycerol, 0.1M and 0.05M were evaluated with 0.1 g/L of Fe-PILC (Fig. 6). It can be observed that the production rate of both, DHA and GCD, directly depends on

glycerol initial concentration. This is expected since a higher amount of glycerol will also lead to a higher concentration of hydrogen peroxide and if there is the right amount of catalyst, such hydrogen peroxide will be readily dissociated thus originating the oxidant species to increase the glycerol oxidation rate which is translated into a higher production of DHA.

4. Conclusions

Iron pillared clay (Fe-PILC) can be used to enhance the selectivity of the glycerol photo-oxidation towards dihydroxyacetone (DHA) or glyceraldehyde (GCD). Hydrogen peroxide is produced during such a reaction. Therefore, the production of DHA is plausible to be due to the oxidation of glycerol via the generated hydroxyl radicals produced by the dissociation of the *in situ* produced H_2O_2. The production rate and selectivity towards DHA is higher with Fe-PILC than with the typical photocatalyst TiO_2.

Acknowledgements

Arisbeht Mendoza acknowledges CONACYT for financial support to conduct postgraduate studies, CONAYCT project 269093 and UAEM project 4373 are also acknowledged. Authors are grateful to Alejandra Núñez Pineda, Citlalit Martínez Soto, Uvaldo Hernandez Balderas, Lourdes Hurtado and Deysi Amado Piña for technical support.

References

[1] A. Demirbas, Biodiesel : a realistic fuel alternative for diesel engines, Springer-V, London, 2008.

[2] OECD-FAO, OECD-FAO Agricultural Outlook 2014–2023-Commodity Database (OECD, Paris, 2015)., 2014. doi:dx.doi.org/10.1787/agr_outlook-2012-en.

[3] M. Ayoub, A.Z. Abdullah, Critical review on the current scenario and significance of crude glycerol resulting from biodiesel industry towards more sustainable renewable energy industry, Renew. Sustain. Energy Rev. 16 (2012) 2671–2686. doi:10.1016/j.rser.2012.01.054.

[4] Farm Energy, New Uses for Crude Glycerin from Biodiesel Production, EXtension. (2012) 20–23. doi:10.3390/su9101734.

[5] L. GONG, Y. LÜ, Y. DING, R. LIN, J. LI, W. DONG, T. WANG, W. CHEN, Solvent Effect on Selective Dehydroxylation of Glycerol to 1,3-Propanediol over a Pt/WO3/ZrO2 Catalyst, Chinese J. Catal. 30 (2009) 1189–1191. doi:10.1016/S1872-2067(08)60142-4.

[6] J. Xu, Y. Zhao, H. Xu, H. Zhang, B. Yu, L. Hao, Z. Liu, Selective oxidation of glycerol to formic acid catalyzed by Ru(OH)4/r-GO in the presence of FeCl3, Appl. Catal. B Environ. 154–155 (2014) 267–273. doi:10.1016/j.apcatb.2014.02.034.

[7] Y. Jun Choi, J. Hwan Park, T. Yong Kim, S. Yup Lee, Metabolic engineering of Escherichia coli for the production of 1-propanol, Metab. Eng. 14 (2012) 477–486. doi:10.1016/j.ymben.2012.07.006.

[8] F.D. Elziebeta Skrzynska, Anna Wondolowska-Grabowska, Mickaël Capron, Crude glycerol as a raw material for the liquid phase oxidation reaction, 482 (2014) 245–257. doi:10.1016/j.apcata.2014.06.005.

[9] P.U. Okoye, B.H. Hameed, Review on recent progress in catalytic carboxylation and acetylation of glycerol as a byproduct of biodiesel production, Renew. Sustain. Energy Rev. 53 (2016) 558–574. doi:10.1016/j.rser.2015.08.064.

[10] A. Behr, J. Eilting, K. Irawadi, J. Leschinski, F. Lindner, Improved utilisation of renewable resources: New important derivatives of glycerol, Green Chem. 10 (2008) 13–30. doi:10.1039/b710561d.

[11] T. Jedsukontorn, V. Meeyoo, N. Saito, M. Hunsom, Effect of electron acceptors H2O2and O2on the generated reactive oxygen species1O2and OH·in TiO2-catalyzed photocatalytic oxidation of glycerol, Cuihua Xuebao/Chinese J. Catal. 37 (2016) 1975–1981. doi:10.1016/S1872-2067(16)62519-6.

[12] J.A. Sullivan, S. Burnham, The selective oxidation of glycerol over model Au / TiO 2 catalysts — The in fl uence of glycerol purity on conversion and product selectivity, CATCOM. 56 (2014) 72–75. doi:10.1016/j.catcom.2014.06.026.

[13] E. Martin Del Campo, R. Romero, G. Roa, E. Peralta-Reyes, J. Espino-Valencia, R. Natividad, Photo-Fenton oxidation of phenolic compounds catalyzed by iron-PILC, Fuel. 138 (2014) 149–155. doi:10.1016/j.fuel.2014.06.014.

[14] J.L. Valverde, A. Romero, R. Romero, P.B. García, M.L. Sánchez, I. Asencio, Preparation and characterization of Fe-PILCS. Influence of the synthesis parameters, Clays Clay Miner. 53 (2005) 613–621. doi:10.1346/CCMN.2005.0530607.

[15] M. Luo, D. Bowden, P. Brimblecombe, Applied Catalysis B : Environmental Catalytic property of Fe-Al pillared clay for Fenton oxidation of phenol by H 2 O 2, 85 (2009) 201–206. doi:10.1016/j.apcatb.2008.07.013.

[16] C. Catrinescu, D. Arsene, P. Apopei, C. Teodosiu, Degradation of 4-chlorophenol from wastewater through heterogeneous Fenton and photo-Fenton process , catalyzed by Al – Fe PILC, Appl. Clay Sci. 58 (2012) 96–101. doi:10.1016/j.clay.2012.01.019.

[17] T. Undabeytia, M.C. Galán-jiménez, E. Gómez-pantoja, J. Vázquez, B. Casal, F. Bergaya, E. Morillo, Fe-pillared clay mineral-based formulations of imazaquin for reduced leaching in

soil, Appl. Clay Sci. 80–81 (2013) 382–389. doi:10.1016/j.clay.2013.07.001.
[18] Q. Chen, P. Wu, Z. Dang, N. Zhu, P. Li, J. Wu, X. Wang, Iron pillared vermiculite as a heterogeneous photo-Fenton catalyst for photocatalytic degradation of azo dye reactive brilliant orange X-GN, Sep. Purif. Technol. 71 (2010) 315–323. doi:10.1016/j.seppur.2009.12.017.
[19] O.B. Ayodele, J.K. Lim, B.H. Hameed, Pillared montmorillonite supported ferric oxalate as heterogeneous photo-Fenton catalyst for degradation of amoxicillin, Appl. Catal. A Gen. 413–414 (2012) 301–309. doi:10.1016/j.apcata.2011.11.023.
[20] B. Iurascu, I. Siminiceanu, D. Vione, M.A. Vicente, A. Gil, Phenol degradation in water through a heterogeneous photo-Fenton process catalyzed by Fe-treated laponite, Water Res. 43 (2009) 1313–1322. doi:10.1016/j.watres.2008.12.032.
[21] T. Jedsukontorn, N. Saito, M. Hunsom, Photocatalytic behavior of metal-decorated TiO2and their catalytic activity for transformation of glycerol to value added compounds, Mol. Catal. 432 (2017) 160–171. doi:10.1016/j.mcat.2017.02.022.
[22] L.F. González-bahamón, D. Fernando, N. Benítez, C. Pulgarín, Chemosphere New Fe-immobilized natural bentonite plate used as photo-Fenton catalyst for organic pollutant degradation, 82 (2011) 1185–1189. doi:10.1016/j.chemosphere.2010.11.071.
[23] N. Klamerth, S. Malato, A. Agüera, A. Fernández-Alba, Photo-Fenton and modified photo-Fenton at neutral pH for the treatment of emerging contaminants in wastewater treatment plant effluents: A comparison, Water Res. 47 (2013) 833–840. doi:10.1016/j.watres.2012.11.008.
[24] M.N. Timofeeva, S.T. Khankhasaeva, Y.A. Chesalov, S. V. Tsybulya, V.N. Panchenko, E.T. Dashinamzhilova, Synthesis of Fe,Al-pillared clays starting from the Al,Fe-polymeric precursor: Effect of synthesis parameters on textural and catalytic properties, Appl. Catal. B Environ. 88 (2009) 127–134. doi:10.1016/j.apcatb.2008.09.013.
[25] G.M. Eisenberg, Colorimetric Determination of Hydrogen Peroxide, Ind. Energineering Chem. 15. No.5 (1943) 327–328.
[26] L. Hurtado, R. Romero, A. Mendoza, S. Brewer, K. Donkor, R.M. Gómez-Espinosa, R. Natividad, Paracetamol mineralization by Photo Fenton process catalyzed by a Cu/Fe-PILC under circumneutral pH conditions, J. Photochem. Photobiol. A Chem. 373 (2019) 162–170. doi:10.1016/j.jphotochem.2019.01.012.
[27] C. Minero, A. Bedini, V. Maurino, Glycerol as a probe molecule to uncover oxidation mechanism in photocatalysis, Appl. Catal. B Environ. 128 (2012) 135–143. doi:10.1016/j.apcatb.2012.02.014.

Figure Captions

Fig.1 X-Ray Diffractogram of Fe-PILC.

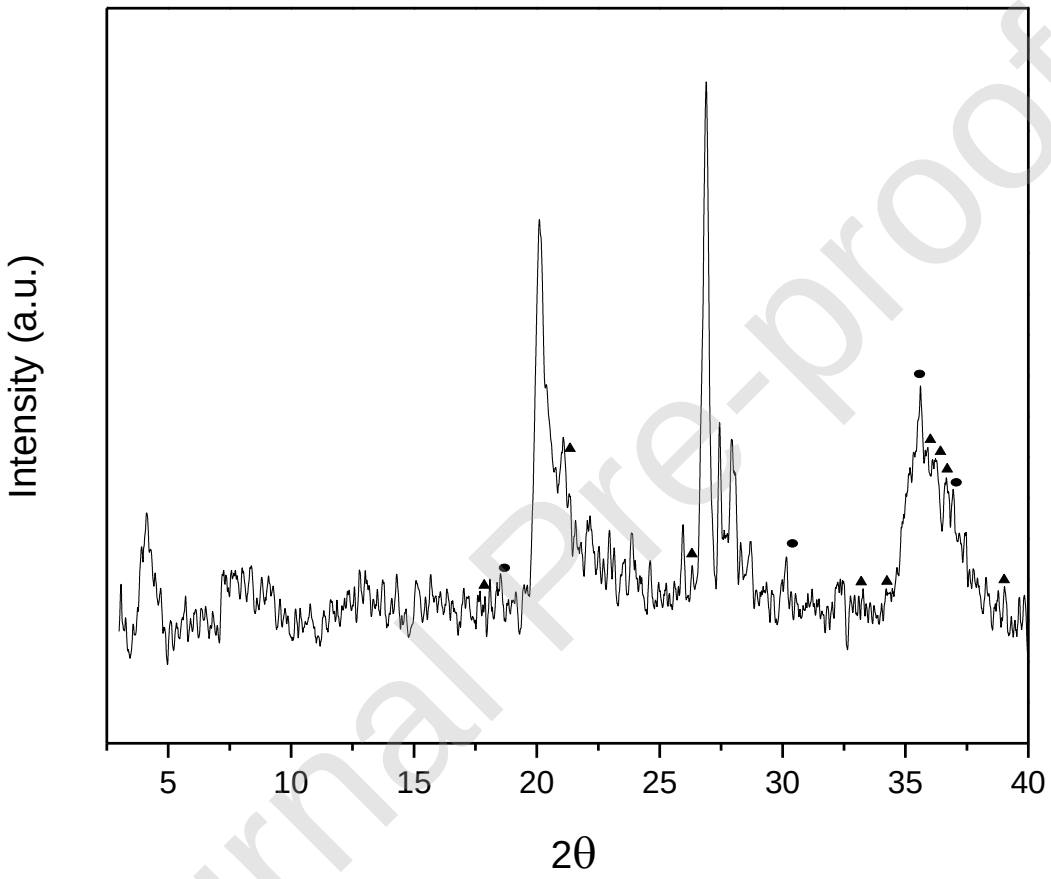

Fig. 1. XRD pattern of Fe-Pilc´s. (•Fe_3O_4 (magnetite) [JCPDS #89-0688], ▲FeO(OH) (goethite) [JCPDS #81-0463])

Fig.2. XPS Spectra of Fe-PILC at Fe $2p_{3/2}$ region.

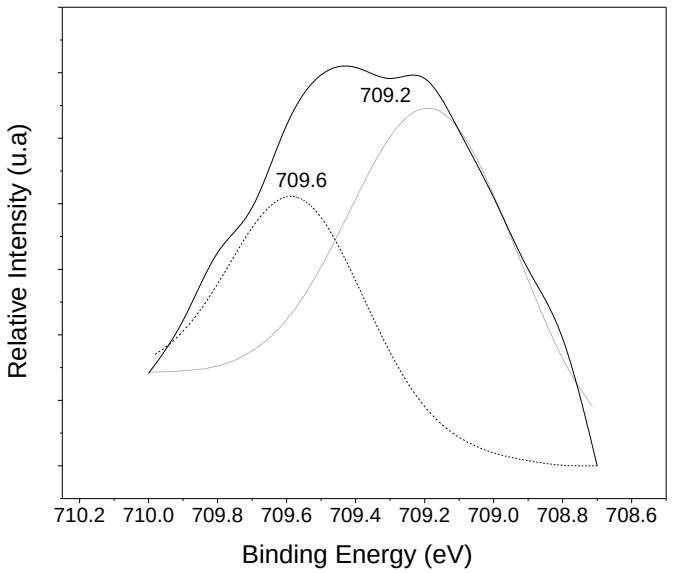

Figure 3. Effect of catalyst loading and catalyst type on a) Dihydroxiacetone, b) Glyceraldehyde evolution with time. Reaction conditions: $[Glycerol]_o$=0.1 M, T=298 K, stirring speed= 1000 rpm.

Fig. 3 a) Effect of catalyst loading on Dihydroxyacetone (DHA) evolution with time. Reaction conditions: $[Glycerol]_o$= 0.1 M, T= 298 K, UV wavelength= 254 nm, 1000 r/min.

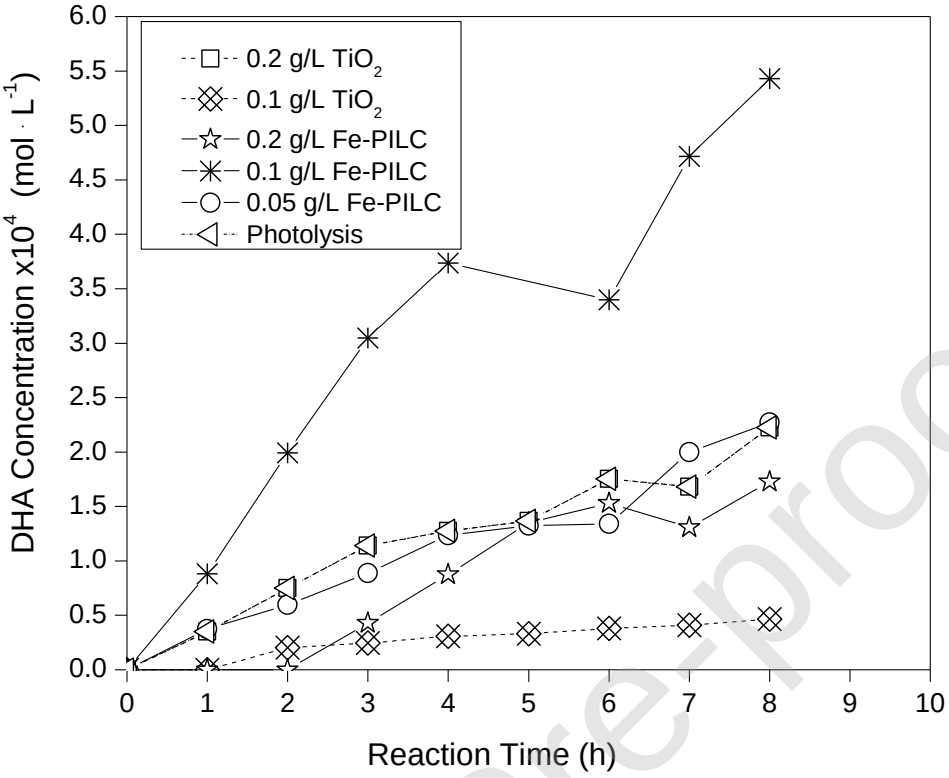

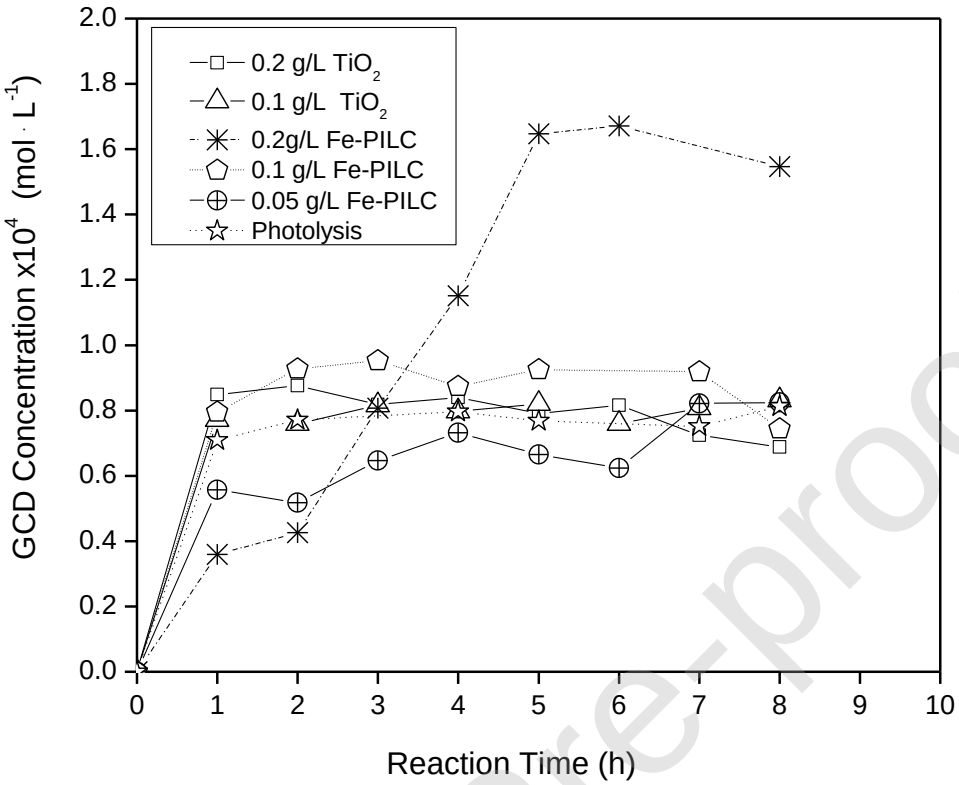

Fig. 3. Effect of catalyst loading on a) Dihydroxiacetone (DHA), b) Glyceraldehyde (GCD) evolution with time. Reaction conditions: $[Glycerol]_o$=0.1 M, T= 298 K, UV wavelength= 254 nm, 1000 rpm.

Fig. 4. H_2O_2 evolution. Experimental conditions: $[Glycerol]_0$= 0.1M, stirring speed=1000 rpm, UV wavelength=254nm, T=298 K, $W_{Fe\text{-}PILC}$=0.2 g/L.

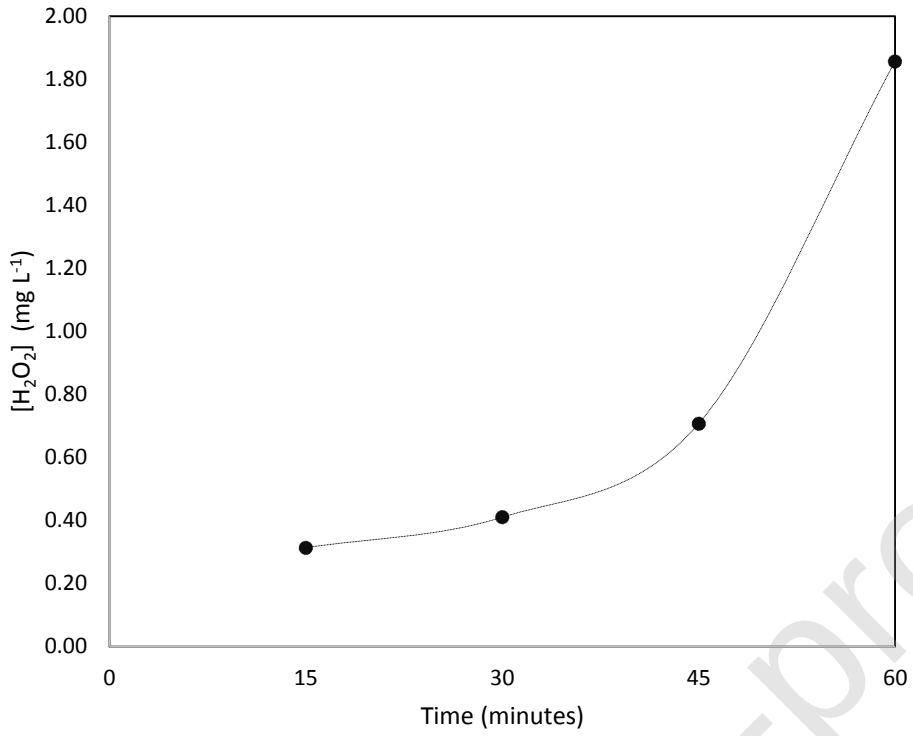

Figure 5. Effect of Fe-PILC loading, catalyst type and reaction time on selectivity towards a) DHA and b) GCD. Reaction conditions: $[Glycerol]_o$=0.1 M, T=298 K, stirring speed= 1000 rpm.

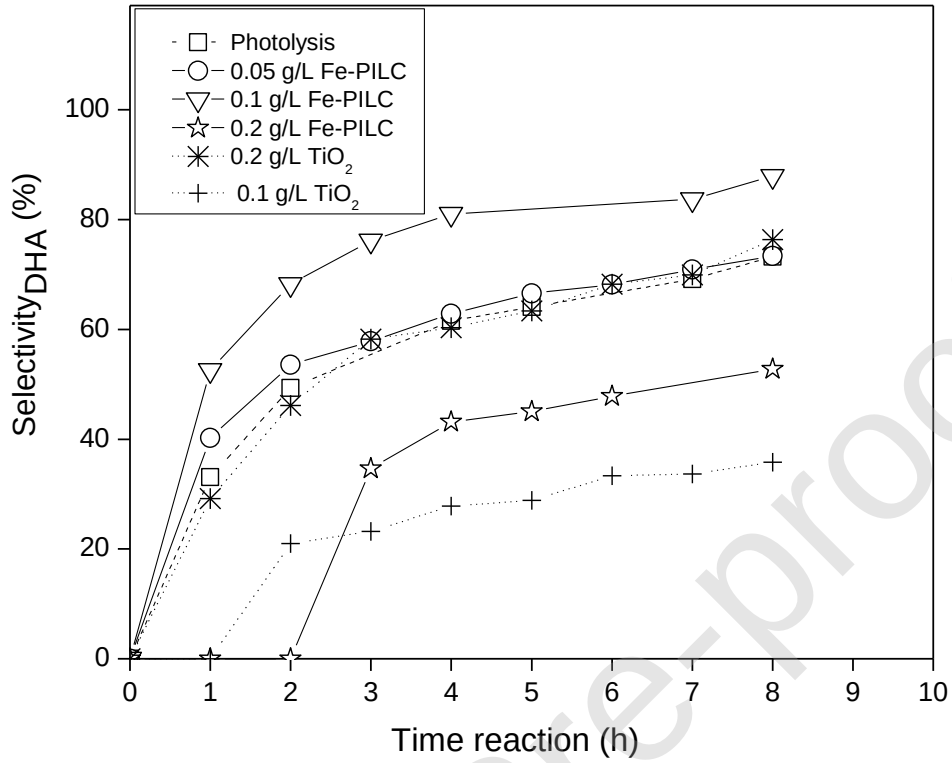

(a)

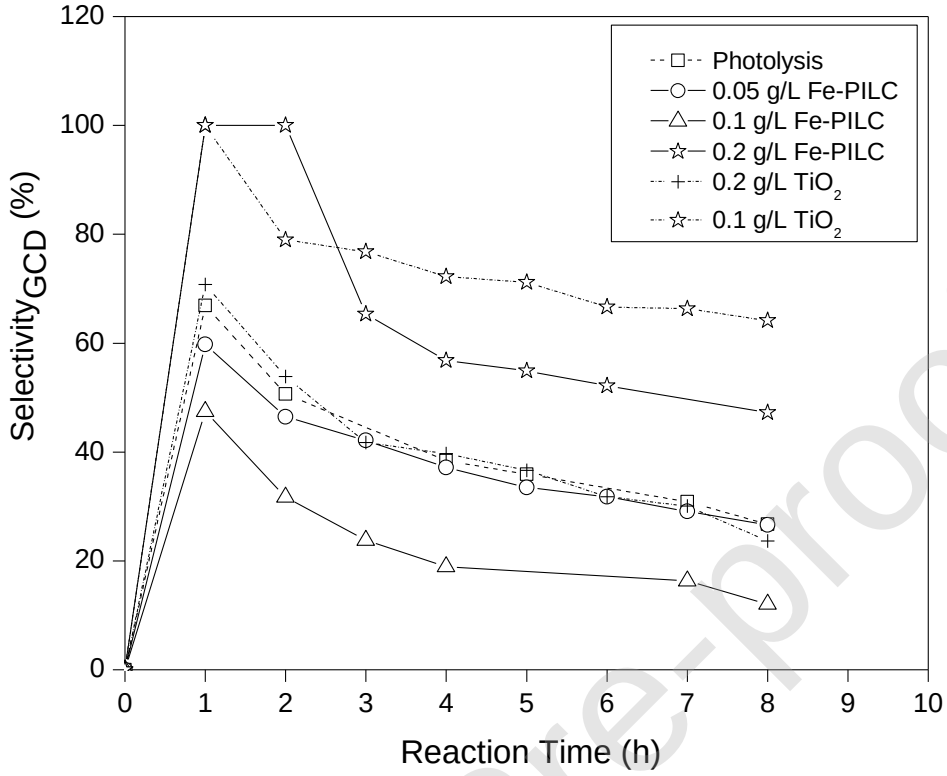

(b)

Fig. 5 Effect of catalyst loading and type, and reaction time on selectivity towards a) Dydroxyacetone (DHA), b) Glyceraldehyde (GCD). Reaction conditions: $[Glycerol]_o$ = 0.1 M, UV wavelength= 254 nm, 1000 rpm, T= 298 K ± 2.

Fig. 6. Effect of initial glycerol concentration on GCD and DHA temporal profiles. Reaction conditions: stirring speed=1000 rpm, UV wavelength=254nm, Fe-PILC loading= (0.1 g/L) and T=298 K.

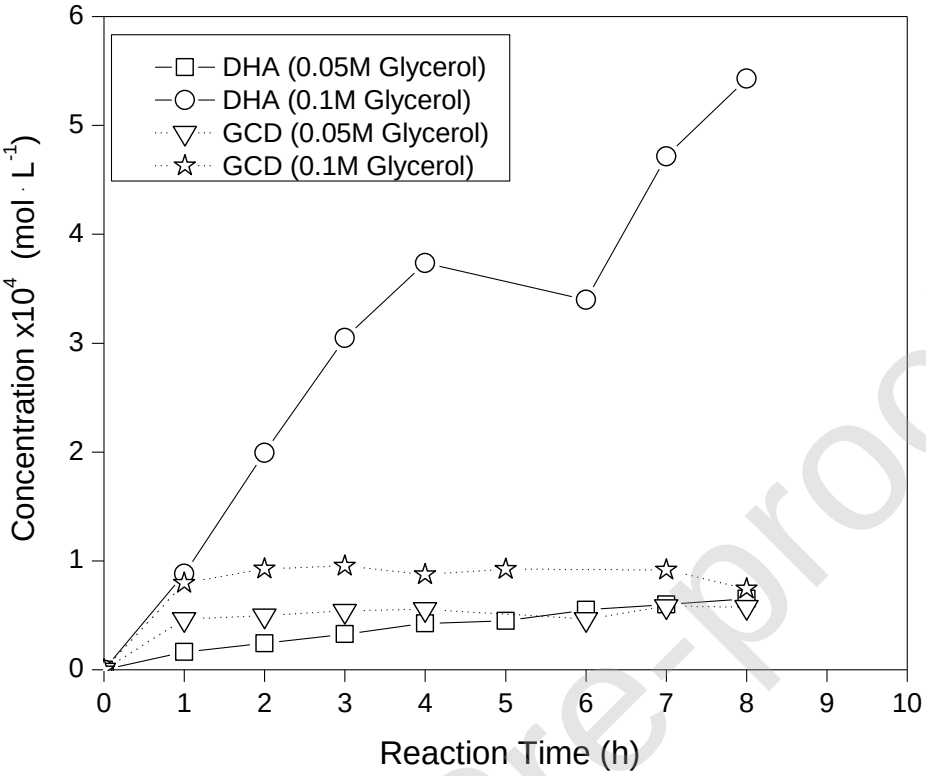

Fig. 6. Concentration of GCD and DHA as a function of initial concentration of Glycerol catalyzed with Fe-PILC. Reaction conditions: UV wavelength= 254 nm, T=298 K ±2, 1000 rpm, Wcat=0.1 g/L

Scheme 1. Glycerol photo-oxidation reaction scheme.